MOLECULAR MECHANISM OF ENSITRELVIR AND ITS SIMILARITY INHIBITING SARS-COV-2 MAIN PROTEASE BY MOLECULAR DYNAMICS SIMULATION

Huynh Thi Ngoc Thanh[1], Kieu Minh Nhan[2,3], Kieu Nhat Ha[3], and Nguyen Quoc Thai[3*]

[1]IT and Lab Center, Dong Thap University, Cao Lanh 870000, Vietnam

[2]Office of Facilities and Project Management, Dong Thap University, Cao Lanh 870000, Vietnam

[3]Division of Physics, School of Education, Dong Thap University, Cao Lanh 870000, Vietnam

[*]Corresponding author: Nguyen Quoc Thai, Email: nqthai@dthu.edu.vn

Article history

Received: 15/3/2024; Received in revised form: 05/4/2024; Accepted: 23/5/2024

Abstract

The unprecedented challenge posed by the COVID-19 pandemic, driven by SARS-CoV-2, has emerged as a global threat. In response, a limited array of therapeutics has been approved for the prevention and treatment of SARS-CoV-2 infection. The main protease (Mpro) of SARS-CoV-2 has been a significant target for drug development efforts because of its crucial role in the viral replication process. This study is to investigate the efficacy of Ensitrelvir and its derivatives in inhibiting the mechanism of the Mpro target of SAR-CoV-2. Docking simulation and molecular dynamic simulation (SMD) techniques were employed for this purpose. The results indicate that the CID 166498740 derivative obtained affinity energy -9.3 kcal/mol and rupture force (F_{max}) 638.3 ± 79.3 (pN), which proved that the CID 166498740 derivative strongly interacted with the Mpro target, emphasizing non-binding interactions as more crucial than hydrogen bonding in stabilizing the receptor-ligand conformation.

Keywords: *Mpro, SARS-CoV-2, Ensitrelvir, derivatives of Ensitrelvir, docking method, SMD method.*

DOI: https://doi.org/10.52714/dthu.13.5.2024.1286

Cite: Huynh, T. N. T., Kieu, M. N., Kieu, N. H., & Nguyen, Q. T. (2024). Molecular mechanism of Ensitrelvir and its similarity inhibiting SARS-CoV-2 main protease by molecular dynamics simulation. *Dong Thap University Journal of Science, 13*(5), 37-44. https://doi.org/10.52714/dthu.13.5.2024.1286.

CƠ CHẾ PHÂN TỬ CỦA ENSITRELVIR VÀ CÁC HỢP CHẤT TƯƠNG ĐỒNG CỦA ENSITRELVIR ỨC CHẾ MAIN PROTEASE CỦA SARS-COV-2 BẰNG MÔ PHỎNG ĐỘNG LỰC PHÂN TỬ

Huỳnh Thị Ngọc Thanh[1], Kiều Minh Nhân[2,3], Kiều Nhật Hạ[3] và Nguyễn Quốc Thái[3*]

[1]Trung tâm Thực hành - Thí nghiệm, Trường Đại học Đồng Tháp, Việt Nam

[2]Phòng Thiết bị và Xây dựng Cơ bản, Trường Đại học Đồng Tháp, Việt Nam

[3]Bộ môn Vật lý, Trường Sư phạm, Trường Đại học Đồng Tháp, Việt Nam

[*]Tác giả liên hệ: Nguyễn Quốc Thái, Email: nqthai@dthu.edu.vn

Article history

Ngày nhận: 15/3/2024; Ngày nhận chỉnh sửa: 05/4/2024; Ngày duyệt đăng: 23/5/2024

Tóm tắt

Đại dịch COVID-19 do SARS-CoV-2 gây ra là mối đe dọa toàn cầu chưa từng có. Để ngăn chặn đại dịch này, một số phương pháp điều trị đã được thực hiện nhằm phòng ngừa và điều trị nhiễm SARS-CoV-2. Main Protease (Mpro) của SARS-CoV-2 là thụ thể quan trọng cho việc phát triển thuốc vì Mpro có vai trò chính trong quá trình nhân lên của virus SARS-CoV-2. Mục đích chính của nghiên cứu này nhằm làm sáng tỏ cơ chế phân tử của Ensitrelvir và các dẫn xuất của nó trong việc ức chế hoạt động thụ thể Mpro của SAR-CoV-2. Bằng phương pháp mô phỏng docking và mô phỏng động lực phân tử định hướng (SMD), kết quả chỉ ra rằng dẫn xuất CID 166498740 của Ensitrelvir có ái lực liên kết là -9.3 kcal/mol và lực bức liên kết cực đại (F_{max}) CID 166498740 là 638.3 ± 79.3 (pN), điều này chứng minh rằng CID 166498740 tương tác mạnh với thụ thể Mpro, đặc biệt khi xác định tính ổn định cấu hình của hệ phối tử-thụ thể cho thấy rằng tương tác không liên kết có vai trò quan trọng hơn liên kết hydrogen.

Từ khóa: *Mpro, SARS-CoV-2, Ensitrelvir, derivatives of Ensitrelvir, docking method, SMD method.*

1. Introduction

The emergence of SARS-CoV-2 has presented a global challenge, driving the COVID-19 pandemic. While some treatments, such as vaccines, monoclonal antibodies, and compounds targeting key viral enzymes (He et al., 2023), have been authorized for combating the virus, the enduring nature of the pandemic coupled with the inherent mutability of RNA viruses allows SARS-CoV-2 to generate diverse mutations. These mutations may lead to the emergence of variant strains, potentially undermining the effectiveness of current therapies (Davies et al., 2021). By January 2024, The World Health Organization (WHO) reported more than 750 million cases and killed over 7 million of people in all over the world.

The genetic structure of SARS-CoV-2 closely resembles that of SARS-CoV, sharing 96% of its entire genome originating from a bat coronavirus within the beta genus of the coronavirus family (Gorbalenya et al., 2020; Zhou et al., 2020). Both coronavirus genomes have a glycosylated spike protein (S) as a pivotal component. This protein facilitates the binding of both SARS-CoV and SARS-CoV-2 to the angiotensin-converting enzyme 2 (ACE2), a protein situated on the surface membrane of host cells. Furthermore, the SAR-CoV-2 genome contains numerous non-structural proteins, such as the coronavirus main protease (Mpro), papain-like protease (PLpro), and RNA-dependent RNA polymerase (RdRp). These proteins, termed NSPs, are crucial for viral replication. Main protease, also known as 3-chymotrypsin-like protease (3CLpro), is a viral cysteine protease essential for this process (Mondal et al., 2022). Upon entering the host cell, the positive-sense single-stranded viral RNA genome is translated by the host ribosome, producing two long polyproteins named pp1a and pp1ab. These polyproteins are then cleaved proteolytically to generate various NSPs required for subsequent stages of the viral life cycle (Mondal et al., 2022). Mpro plays a crucial role as it cleaves polyproteins at a minimum of 11 conserved sites.

Nirmatrelvir and Ensitrelvir were two oral antiviral drugs targeting Mpro that received emergency use authorization (EUA). Nirmatrelvir exhibited a more substantial decrease in the likelihood of hospitalization and mortality compared to a placebo (Owen et al., 2021). Following a phase 2/3 clinical trial demonstrating swift clearance of SARS-CoV-2, Ensitrelvir obtained emergency authorization in Japan for treatment (Mukae et al., 2022; Unoh et al., 2022).

In this study, we combined screening virtual, docking and molecular dynamic simulation (SMD) to sifting similarity compounds and calculate their potential interaction with Mpro. We have screened 81 compounds with 85% similarity Ensitrelvir from PubChem, and then used docking method to obtain 02 compounds has the binding energy lower -9.3 kcal.mol^{-1}.

2. Material and Methods

2.1. The ligands and main protease (Mpro) target

The structure of Ensitrelvir and its similarities were taken from PubChem data bank (Kim et al., 2022). CID of Ensitrelvir is 162533924 which 3D conformations are presented in Figure 1. The molecular formula of Ensitrelvir is $C_{22}H_{17}ClF_3N_9O_2$.

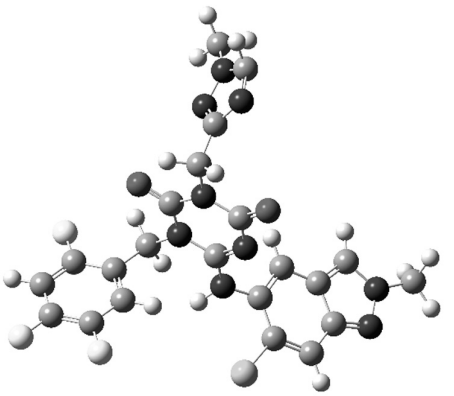

Figure 1. The 3D structure of Ensitrelvir

The structure of main protease target (Mpro) with the binding site of Ensitrelvir was obtained from Protein Data Bank (PDB) with 8HBK (Duan et al., 2023), It showed in Figure 2.

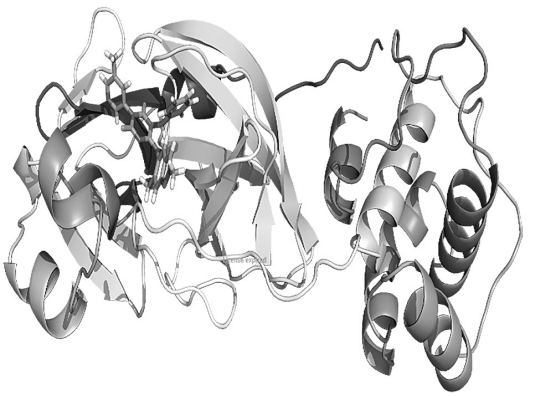

Figure 2. The crystal structure of SARS-CoV-2 3CL protease in complex with Ensitrelvir

2.2. Methods

2.2.1. Docking method

The Mpro target (8HBK) and Ensitrelvir and its derivatives converted to PDBQT files by AutoDock Tool 1.5.4 (Sanner, 1999). The Autodock Vina version 1.1 (Trott & Olson, 2010) was utilized for docking simulation that docked ligands to target. To facilitate a thorough global search, ensuring robust results the exhaustiveness parameter was configured at 400. The dynamics of receptor atoms were disregarded. Twenty binding modes were produced, initialized from random ligand configurations with complete flexibility in torsion angles. The box was chosen big enough to cover the binding site of target with size_x = 25.0, size_y = 20.0, size_z = 20.0 and center_x = -21.75, center_y = -11.26, center_z = 2.66.

2.2.2. Measures used in data analysis

A hydrogen bond (HB) arises when the distance between the donor (D) and acceptor (A) is less than 0.35 nm, with the H-A distance below 0.27 nm, and the D-H-A angle surpassing 135 degrees. Non-bonded contact between the ligand and receptor residue occurs when their centers of mass are within 0.65 nm of each other. (Thai et al., 2018).

2.2.3. Steered molecular dynamics

The Steered Molecular Dynamics (SMD) method was developed to investigate the mechanical unfolding of biomolecules (Israelewitz et al., 2001; Kumar & Li, 2010) and the unbinding of ligands from receptors along a specified direction (Grubmüller et al., 1996). The pulling direction was employed to determine the optimal path for the ligand's exit from the receptor, acting as the pulling direction by the MSH method (Vuong et al., 2015) utilizes a constant loading speed v applied to the dummy atom with a force $F = k(\Delta z - vt)$, where Δz represents the displacement of the pulled atom from its initial position. A harmonic potential with a spring constant $1000 kJ.nm^{-1}.mol^{-1}$ was applied to the C-alpha atoms to maintain the overall structure of target (Thai et al., 2017).

In this study, the pulling rate is $0.001 nm.ps^{-1}$ and the pulling constant is 600kJ/nm/mol. The pulling force put on the center of mass of Ensitrelvir and its derivatives with the direction along the z axis. Within the SMD methodology, the maximum force, denoted as F_{max}, within the force-extension/time profile serves as a metric for assessing binding affinity. A higher F_{max} indicates a stronger binding of the ligand (Thai et al., 2017).

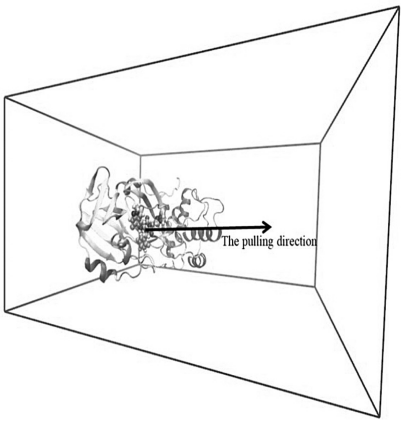

Figure 3. The pulling direction of Ensitrelvir was obtained by MSH

3. Results and discussion

3.1. Docking scores and best docking poses

From PubChem data bank screened 81 compounds with 85% similarity Ensitrelvir (Vuong et al., 2013). The docking binding energy of Ensitrelvir with Mpro is -9.3 $kcal.mol^{-1}$ in Table 1 for the best docking mode implied that Ensitrelvir strongly binds into Mpro. The in vitro experiment showed that the IC_{50} value of Ensitrelvir for SARS-CoV-2 is 0.049 ± 0.001 μM (Lin et al., 2023). Using the formula $\Delta G_{exp} = RTln(IC_{50})$, where gas constant $R = 1.987 \times 10^{-3}$ $kcal.mol^{-1}$, T = 300K, and IC_{50} is measured in M, the result of experiment was obtained $\Delta G_{exp} = -10.03$ $kcal.mol^{-1}$, this observation roughly aligns with the outcomes obtained from our docking analysis. Compare that to the binding energy close to -9.3 kcal/mol, the result of docking method for data PubChem was taken 02 compounds. The binding position showed in figure 3 and the binding energy of best docking model presented in Table 1.

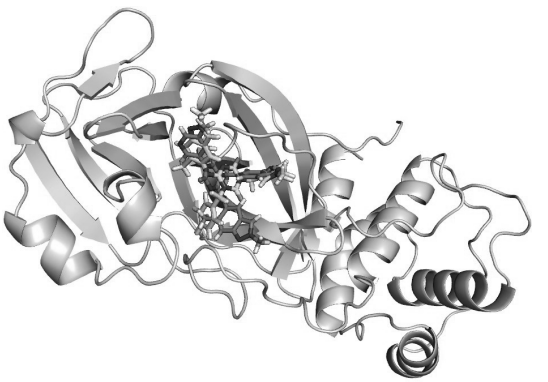

Figure 3. The binding sites of Ensitrelvir and similarity Ensitrelvir in complexes with main protease for the best mode of docking simulation

Table 1. The Ensitrelvir and similarity Ensitrelvir bind into hole of the binding site of Mpro for best docking model

Main protease (8HBK)	ΔE_{bind} (kcal.mol^{-1})	Computed Properties	IC50 (μM)
CID 162623517 (Abimtrelvir)	-9.3	+ Molecular Weight: 527.9 g/mol, + XLogP3-AA: 3.8 + Hydrogen Bond Donor Count: 1 + Hydrogen Bond Acceptor Count: 7 + Topological Polar Surface Area: 95.7Å²	+ 0.014 (For SARS-CoV-2 main protease). (https://pubchem. cbi.nlm.nih. gov/compound/162623517)
CID 166498740	-9.4	+ Molecular Weight: 531.9g/mol, + XLogP3-AA: 2.2 + Hydrogen Bond Donor Count: 1 + Hydrogen Bond Acceptor Count: 8 + Topological Polar Surface Area: 114Å²	Invaluable for the main SARS-CoV-2 protease (https://pubchem.cbi.nlm.nih. gov/compound/166498740)

3.2. The binding energy and Hydrogen bonding plays a minor role

From Table 1, the values of binding energy obtained correctly reflects what was shown by experiments. CID 166498740 compound is strongest, which is -9.4 kcal.mol^{-1} while CID 162623517 and Ensitrelvir is nearly, -9.3 kcal.mol^{-1}.

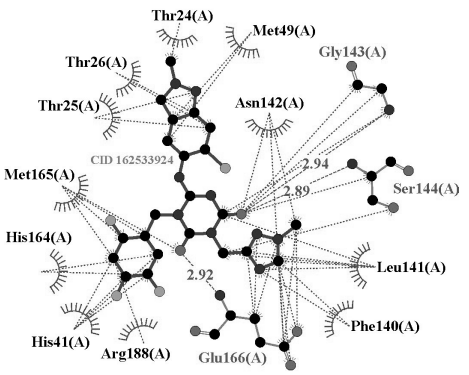

Figure 4A. The hydrogen bond (HB) is in green, non-bonded contact (NBC) is in red lines of CID 162533924

Using LigPlot+ version 1.4.4, hydrogen bonds (HBs) and non-bonded contacts (NBCs) networks of CID 162623517, CID 166498740 and Ensitrelvir shown in Figure 4A-C, which has been prepared by the parameters in 2.2.2 (Measures used in data analysis). CID 166498740 has 13 non-bonded contacts and 03 hydrogen bonds (Glu166(A), Gly143(A), Cys145(A) with Mpro, corresponding to binding energy -9.4 kcal. mol^{-1}. This also occurs with Ensitrelvir but the number of nonbonded contacts is less than 2. Meanwhile, CID 162623517 has the binding energy -9.3 kcal.mol^{-1} but with 08 nonbonded contacts and 02 hydrogen bonds (Gly143(A), Ser144(A). These findings indicate that the non-bonded contact network is more extensive than the hydrogen bond network, suggesting that hydrogen bonding exerts a less significant role in stabilizing receptor-ligand complexes compared to non-bonded interactions.

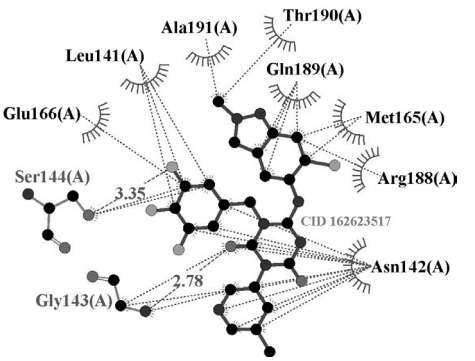

Figure 4B. The hydrogen bond (HB) is in green, non-bonded contact (NBC) is in red lines of CID 166498740

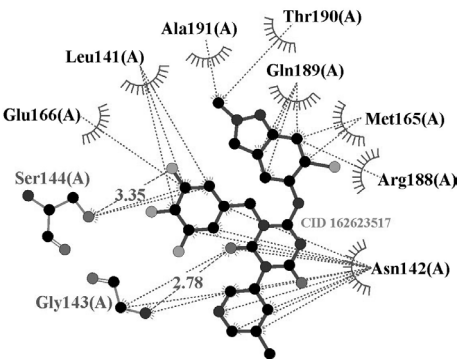

Figure 4C. The hydrogen bond (HB) is in green, non-bonded contact (NBC) is in red lines of CID 162623517

Table 2. List of SARS-COV-2 main protease target residues forming non-bonded contact with CID 162533924 (Ensitrelvir), CID 162623517, CID 166498740.

Compounds	NBCs	Amino acids
Ensitrelvir (CID 162533924)	11	Arg188(A), His41(A), His164(a), Met165(A), Thr25(A), Thr26(A), Thr24(A), Met49(A), Asn42(A), Leu141(A), Phe140(A).
CID 162623517	08	Glu166(A), Leu141(A), Ala191(A), Thr190(A), Gln189(A), Met165(A), Arg188(A), Asn142(A).
CID 166498740	13	His163(A), Arg188(A), His41(A), Met165(A), His164(A), Met49(A), Thr24(A), Thr26(A), Thr25(A), Phe140(A), Asn142(A), Leu141(A), Ser144(A).

3.3. The result SMD

The docking method, while useful, isn't always precise due to its limitations. These include overlooking receptor dynamics and a restricted range of ligand positions for trial. To address this, we opted to identify the docking energies with the lowest values and then enhance their binding affinity through the SMD method. Because SMD method, a higher rupture force (F_{max}) indicates stronger binding. Our study aims to select compounds with F_{max} values surpassing those of a reference compound known for its high binding affinity, as established in the experiment.

We utilized the final snapshot obtained at equilibrium from the standard MD simulation as the initial conformation for the subsequent SMD simulation. Given the sensitivity of the force time/displacement profile to SMD runs, we conducted 10 independent trajectories, each starting from the same initial configuration but with different seed numbers. The rupture force results were then averaged over these 10 runs to obtain the final outcomes.

From Figure 5 and Figure 6, the time-dependent force was displayed by the ligand during the SMD simulation for three Mpro-ligand complexes.

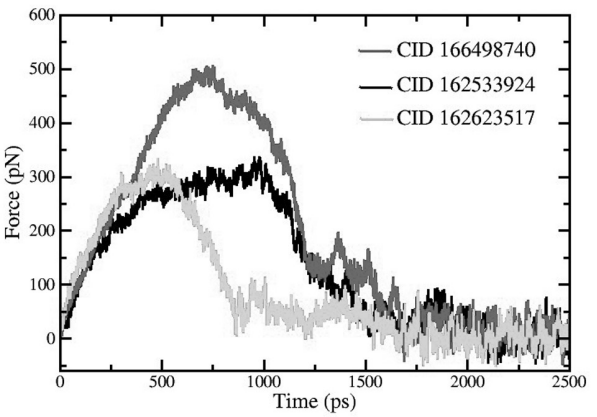

Figure 5. The time dependence of the force experienced by three ligands during SMD simulation

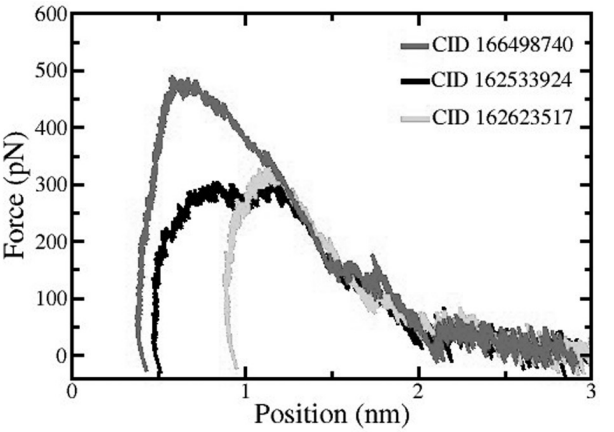

Figure 6. The position dependence of the force experienced by three ligands during SMD simulation

The overall observation is that F_{max} varies across different time scales depending on the systems under study. Averaging the rupture force over 10 trajectories, the results indicate that for the target Mpro, CID 166498740 exhibits a higher rupture force (F_{max}) compared to the rupture force of Ensitrelvir. This result is conformed with the result docking, however, the higher rupture force (F_{max}) of CID 162623517 is the lowest in spite of the docking method which is ranked nearly CID 162533924. The result SMD is showed in Table 3.

From table 3, the rupture force (F_{max}) of CID 162623517 is 638.3 ± 79.3 (pN), which is higher than the rupture force (F_{max}) of Ensitrelvir (475.9 ± 53.8 (pN)). This mean that CID 162623517 inhibits the Mpro receptor better than Ensitrelvir. The results confirm that these compounds exhibit inhibition constants in the micromolar range. Therefore, we propose that compound CID 162623517 needs to be studied further, using more precise methods.

Table 3. The ranking of rupture force (F_{max}) was obtained by SMD method

No.	CID 162533924/ F_{max}(pN)	CID 162623517/ F_{max}(pN)	CID 166498740/ F_{max}(pN)
1	470.2	282.5	742.9
2	511.0	297.8	868.8
3	543.4	311.8	493.9
4	548.5	304.8	519.5
5	484.6	269.6	542.0
6	633.8	334.5	822.4
7	448.6	295.3	583.0
8	407.5	350.0	505.0
9	306.1	295.8	667.5
10	404.8	294.9	638.1
Average	475.9 ± 53.8	303.7 ± 13.8	638.3 ± 79.3

4. Conclusions

Through a series of sequential screenings involving virtual screening, docking, and SMD simulation, we have predicted 01 compound (CID 166498740) which can inbibit the SARS-COV-2 main protease target better than conference compound Ensitrelvir with IC_{50} equal 0.049 ± 0.001 μM. By docking method, the predominant factor influencing binding affinity is the non-bonded contacts interactions, with hydrogen bonding playing a secondary role that is not pivotal. The simultaneously SMD method obtainted rupture force (F_{max}) of CID 166498740 is a better conference compound Ensitrelvir. We highly suggest conducting additional *in vitro* and *in vivo* studies on these compounds.

Acknowledgement: This research is supported by the project B2024-SPD-09.

References

Davies, N. G., Abbott, S., Barnard, R. C., Jarvis, C. I., Kucharski, A. J., Munday, J. D., Pearson, C. A., Russell, T. W., Tully, D. C., & Washburne, A. D. (2021). Estimated transmissibility and impact of SARS-CoV-2 lineage B. 1.1. 7 in England. *Science*, *372*(6538), eabg3055.

Duan, Y., Zhou, H., Liu, X., Iketani, S., Lin, M., Zhang, X., Bian, Q., Wang, H., Sun, H., Hong, S. J., Culbertson, B., Mohri, H., Luck, M. I., Zhu, Y., Liu, X., Lu, Y., Yang, X., Yang, K., Sabo, Y., Chavez, A., Goff, S. P., Rao, Z., Ho, D. D., & Yang, H. (2023). Molecular mechanisms of SARS-CoV-2 resistance to nirmatrelvir. *Nature*, *622*(7982), 376-382. https://doi.org/10.1038/s41586-023-06609-0

Gorbalenya, A. E., Baker, S. C., Baric, R. S., de Groot, R. J., Drosten, C., Gulyaeva, A. A., Haagmans, B. L., Lauber, C., Leontovich, A. M., Neuman, B. W., Penzar, D., Perlman, S., Poon, L. L. M., Samborskiy, D. V., Sidorov, I. A., Sola, I., Ziebuhr, J., & Coronaviridae Study Group of the International Committee on Taxonomy of, V. (2020). The species Severe acute respiratory syndrome-related coronavirus: classifying 2019-nCoV and naming it SARS-CoV-2. *Nature Microbiology*. https://doi.org/10.1038/s41564-020-0695-z

Grubmüller, H., Heymann, B., & Tavan, P. (1996). Ligand binding: molecular mechanics calculation of the streptavidin-biotin rupture force. *Science*, *271*(5251), 997-999.

He, X., He, C., Hong, W., Yang, J., & Wei, X. (2023). Research progress in spike mutations of SARS-CoV-2 variants and vaccine development. *Medicinal Research Reviews*, *43*(4), 932-971.

Israelewitz, B., Gao, M., & Schulten, K. (2001). Steered molecular dynamics and mechanical functions of proteins. *Current Opinion in Structural Biology*, *11*(2), 224-230.

Kim, S., Chen, J., Cheng, T., Gindulyte, A., He, J., He, S., Li, Q., Shoemaker, B. A., Thiessen, P. A., Yu, B., Zaslavsky, L., Zhang, J., & Bolton, E. E. (2022). PubChem 2023 update. *Nucleic Acids Research*, *51*(D1), D1373-D1380. https://doi.org/10.1093/nar/gkac956

Kumar, S., & Li, M. S. (2010). Biomolecules under mechanical force. *Physics Reports*, *486*(1), 1-74.

Lin, M., Zeng, X., Duan, Y., Yang, Z., Ma, Y., Yang, H., Yang, X., & Liu, X. (2023). Molecular mechanism of ensitrelvir inhibiting SARS-CoV-2 main protease and its variants. *Communications Biology*, *6*(1), 694.

Mondal, S., Chen, Y., Lockbaum, G. J., Sen, S., Chaudhuri, S., Reyes, A. C., Lee, J. M., Kaur, A. N., Sultana, N., & Cameron, M. D. (2022). Dual inhibitors of main protease (MPro) and Cathepsin L as potent antivirals against SARS-

CoV-2. *Journal of the American Chemical Society*, *144*(46), 21035-21045.

Mukae, H., Yotsuyanagi, H., Ohmagari, N., Doi, Y., Imamura, T., Sonoyama, T., Fukuhara, T., Ichihashi, G., Sanaki, T., & Baba, K. (2022). A randomized phase 2/3 study of ensitrelvir, a novel oral SARS-CoV-2 3C-like protease inhibitor, in Japanese patients with mild-to-moderate COVID-19 or asymptomatic SARS-CoV-2 infection: results of the phase 2a part. *Antimicrobial Agents and Chemotherapy*, *66*(10), e00697-00622.

Owen, D. R., Allerton, C. M., Anderson, A. S., Aschenbrenner, L., Avery, M., Berritt, S., Boras, B., Cardin, R. D., Carlo, A., & Coffman, K. J. (2021). An oral SARS-CoV-2 Mpro inhibitor clinical candidate for the treatment of COVID-19. *Science*, *374*(6575), 1586-1593.

Sanner, M. F. (1999). Python: a programming language for software integration and development. *Journal of Molecular Graphics and Modelling*, *17*(1), 57-61.

Thai, N. Q., Nguyen, H. L., Linh, H. Q., & Li, M. S. (2017). Protocol for fast screening of multi-target drug candidates: Application to Alzheimer's disease. *Journal of Molecular Graphics and Modelling*, *77*, 121-129. https://doi.org/https://doi.org/10.1016/j.jmgm.2017.08.002

Thai, N. Q., Nguyen, N. Q., Nguyen, C., Nguyen, T. Q., Ho, K., Nguyen, T. T., & Li, M. S. (2018). Screening potential inhibitors for cancer target LSD1 from natural products by steered molecular dynamics. *Molecular Simulation*, *44*(4), 335-342.

Trott, O., & Olson, A. J. (2010). AutoDock Vina: improving the speed and accuracy of docking with a new scoring function, efficient optimization, and multithreading. *Journal of Computational Chemistry*, *31*(2), 455-461.

Unoh, Y., Uehara, S., Nakahara, K., Nobori, H., Yamatsu, Y., Yamamoto, S., Maruyama, Y., Taoda, Y., Kasamatsu, K., Suto, T., Kouki, K., Nakahashi, A., Kawashima, S., Sanaki, T., Toba, S., Uemura, K., Mizutare, T., Ando, S., Sasaki, M., Orba, Y., Sawa, H., Sato, A., Sato, T., Kato, T., & Tachibana, Y. (2022). Discovery of S-217622, a Noncovalent Oral SARS-CoV-2 3CL Protease Inhibitor Clinical Candidate for Treating COVID-19. *Journal of Medicinal Chemistry*, *65*(9), 6499-6512. https://doi.org/10.1021/acs.jmedchem.2c00117

Vuong, Q. V., Nguyen, T. T., & Li, M. S. (2015). A new method for navigating optimal direction for pulling ligand from binding pocket: application to ranking binding affinity by steered molecular dynamics. *Journal of Chemical Information and Modeling*, *55*(12), 2731-2738.

Vuong, Q. V., Siposova, K., Nguyen, T. T., Antosova, A., Balogova, L., Drajna, L., Imrich, J., Li, M. S., & Gazova, Z. (2013). Binding of glyco-acridine derivatives to lysozyme leads to inhibition of amyloid fibrillization. *Biomacromolecules*, *14*(4), 1035-1043.

Zhou, P., Yang, X.-L., Wang, X.-G., Hu, B., Zhang, L., Zhang, W., Si, H.-R., Zhu, Y., Li, B., Huang, C.-L., Chen, H.-D., Chen, J., Luo, Y., Guo, H., Jiang, R.-D., Liu, M.-Q., Chen, Y., Shen, X.-R., Wang, X., Zheng, X.-S., Zhao, K., Chen, Q.-J., Deng, F., Liu, L.-L., Yan, B., Zhan, F.-X., Wang, Y.-Y., Xiao, G.-F., & Shi, Z.-L. (2020). A pneumonia outbreak associated with a new coronavirus of probable bat origin. *Nature*, *579*(7798), 270-273. https://doi.org/10.1038/s41586-020-2012-7